

CrystEngComm

Accepted Manuscript



This is an *Accepted Manuscript*, which has been through the Royal Society of Chemistry peer review process and has been accepted for publication.

Accepted Manuscripts are published online shortly after acceptance, before technical editing, formatting and proof reading. Using this free service, authors can make their results available to the community, in citable form, before we publish the edited article. We will replace this *Accepted Manuscript* with the edited and formatted *Advance Article* as soon as it is available.

You can find more information about *Accepted Manuscripts* in the [Information for Authors](#).

Please note that technical editing may introduce minor changes to the text and/or graphics, which may alter content. The journal's standard [Terms & Conditions](#) and the [Ethical guidelines](#) still apply. In no event shall the Royal Society of Chemistry be held responsible for any errors or omissions in this *Accepted Manuscript* or any consequences arising from the use of any information it contains.

Evaluation of Structural Transformation in 2D Metal–Organic Frameworks Based on 4,4'-Sulfonyldibenzoate Linker: Microwave-Assisted Solvothermal Synthesis, Characterization and Applications†

Cheng-You Wu,^a Duraisamy Senthil Raja,^b Chun-Chuen Yang,^{*c} Chun-Ting Yeh,^a Yu-Ru Chen,^a Chen-Yu Li,^a Bao-Tsan Ko,^{*d} and Chia-Her Lin^{*a}

^aDepartment of Chemistry, Chung Yuan Christian University, Chungli, Taoyuan 320, Taiwan

^bDepartment of Chemistry, National Tsing Hua University, Hsinchu 300, Taiwan

^cDepartment of Physics, Chung Yuan Christian University, Chungli, Taoyuan 320, Taiwan

^dDepartment of Chemistry, National Chung Hsing University, Taichung, 402, Taiwan

Corresponding Authors:

Prof. Chun-Chuen Yang

E-mail: chunchuenyang@cycu.edu.tw

Prof. Bao-Tsan Ko

E-mail: btko@dragon.nchu.edu.tw

Prof. Chia-Her Lin

E-mail: chiaher@cycu.edu.tw

Tel: +886-3-2653315

Fax: +886-3-2653399

Abstract

Six 2D metal-organic frameworks containing V-shaped 4,4'-sulfonyldibenzoate (SBA) linkers, $[\text{Zn}_3(\text{SBA})_2(\text{OH})_2] \cdot \text{EtOH}$ (**1** or **CYCU-5**·EtOH), $[\text{M}_3(\text{OH})_2(\text{SBA})_2(\text{EtOH})(\text{H}_2\text{O})_3] \cdot 3.5\text{H}_2\text{O}$ (**2-4**, M = Mg, Ni, and Co), $[\text{Mn}(\text{SBA})(\text{EtOH})]$ (**5**) and $[\text{Mn}(\text{SBA})(\text{H}_2\text{O})]$ (**6**) have been synthesized rapidly under microwave-assisted solvothermal conditions. The structural analysis revealed that all compounds display two-dimensional structures containing inorganic motifs with one-dimensional chain (**1-5**) or dimer of trigonal prism (**6**) connected through SBA linkers and forming 2D neutral and porous channels. The compounds of **1-4** were further characterized by elemental analysis, thermal gravimetric analyses (TGA), powder X-ray diffraction (PXRD) measurements and IR spectroscopy. The desolvated phases of compounds **1-2/3-4** have thermal stability up to about 400/350 °C. The de-solvated framework of **1-4** after 200 °C have similar **CYCU-5** like conformation and exhibited gas adsorption properties by N_2 , CO_2 and H_2 gases. Interestingly, **CYCU-5** displayed selective CO_2 gas adsorption over N_2 and CH_4 gases at 273 K. In addition, the catalytic ability of **CYCU-5** as an initiator for ring-opening polymerization of L-Lactide has also been demonstrated.

Introduction

Metal–organic frameworks (MOFs) are being intensively studied in recent years because of their fascinating structural diversities and topologies as platforms for various functional applications.^{1,2} They are built up of metal ions interconnected by organic linkers, thus mostly forming two- or three-dimensional porous frameworks. In order to achieve diverse structural MOFs, various routes like room temperature synthesis, conventional electronic heating, microwave heating, electrochemistry, mechano-chemistry, and ultrasonic methods have been employed.³ Particular attention has been paid for microwave-assisted solvothermal reactions, is mainly because of greener approach to synthesize materials in a shorter reaction time with less power consumption than that of conventional solvothermal synthetic method.⁴

It is obvious that the design of MOF materials depend on careful choice of the building blocks such as metal ions, organic linkers, co-ligands, and adequate solvents, and their proper organization in the solid state.⁵ Among them, the selection of organic linkers is one of the significant aspects.⁶ Because, the configuration, rigidity, substituent and coordination modes of organic ligands have played a vital role on determining the structural properties of the MOFs. In this context, V-shaped dicarboxylates as linkers for the construction of MOFs is getting limelight very recently. In particular, 4,4'-sulfonyldibenzoic acid (H₂SBA) is a typical example of a V-shaped dicarboxylate linker for the construction of novel MOFs, as it has six potential donor atoms that allow the formation of variable structural topologies.⁷ In this regard, we have recently been found and published that V-shaped dicarboxylate ligands such as 4,4'-sulfonyldiebenzoate (SBA) and 4,4'-oxybisbenzoate can be used to construct a variety of MOFs having robust structure.⁸

On the other hand, among the MOFs, the 3D frameworks with open channels have largely been known in the recent past, but, relatively few examples of 2D open frameworks are found in the literature.⁹ Further, the 2D MOFs have less been known for their gas sorption properties which is mainly due to the small interlayer spacing between the 2D layers that could not be wide enough for the incorporation of gas molecules.¹⁰ And also, the selective adsorption of CO₂ by using MOFs¹¹ has attracted intensive attention in recent years because CO₂ is believed to be the major greenhouse gas which causes global warming.¹²

With this above background in mind, and, as a continuation of our research on H₂SBA, herein, we report six 2D MOFs, [Zn₃(SBA)₂(OH)₂]·EtOH (**1** or **CYCU-5**·EtOH), [M₃(OH)₂(SBA)₂(EtOH)(H₂O)₃]·3.5H₂O (**2-4**, M = Mg, Ni, and Co), [Mn(SBA)(EtOH)] (**5**) and [Mn(SBA)(H₂O)] (**6**) which are synthesized under microwave-assisted solvothermal conditions. It is

to be noted that the structural description of compound **4** has already been reported,¹³ but, there is no report on its porous properties. Hence, we report its gas sorption properties along with other three new compounds (**1**, **2** and **3**). Further, we report only the single crystal X-ray diffraction structural description for compounds **5** and **6**, because, the yield of both was very low (only very few single crystals have been obtained) for other studies.

Experimental Section

Materials and General Methods

Chemicals of reagent grade or better were used as received. Microwave-assisted reactions were done in a 100 mL Teflon autoclave placed in a microwave oven (START D, Milestone, maximum power of 1200 W, 2.45 GHz) in which the precursor mixtures were heated for several minutes. All products phase purity was examined by powder X-ray diffraction (PXRD) before further characterizations. Elemental analyses were carried out to confirm the composition of the organic part of the prepared samples. Thermal gravimetric analyses (TGA), using a DuPont TA Q50 analyzer, were performed on powder samples under flowing N₂ with a heating rate of 10 °C min⁻¹. FT-IR spectra were recorded in the range of 400-4000 cm⁻¹ on a JASCO FT/IR-460 spectrophotometer using KBr pellets. The gas sorption isotherms have been measured at 77 K for N₂ & H₂, and for CO₂ at 273 & 298 K by using Micromeritics ASAP 2020 adsorption apparatus. About 100 mg of adsorbent has been used for the gas sorption studies. The high pressure gas sorption studies were measured by Quantachrome iSorpHP adsorption system with about 500 mg of each samples. The initial gas removal process was performed under vacuum at 423 K for 12 h. The free space of the system was determined by using He gas. Ultrahigh pure CO₂, N₂, CH₄, H₂ and He gases were used as received in all the gas sorption experiments. Ring-opening polymerization (ROP) of L-lactide (L-LA) catalyzed by **CYCU-5** was carried out by following our previous study.¹⁴

Synthesis of MOFs

Microwave Synthesis of [Zn₃(OH)₂(SBA)₂]·EtOH (1**).** The compound **1** was obtained from a reaction mixture of H₂SBA (0.1224 g, 0.4 mmol), Zn(NO₃)₂·6H₂O (0.2360 g, 0.8 mmol), EtOH (9.0 mL) and H₂O (1.0 mL). The mixture was heated at 180 °C for 40 min. The colorless crystals of **1** were filtered off, washed with EtOH, dried in room temperature atmosphere, and collected with the yield of 0.0782 g (88.41 %, based on the H₂SBA reagent). Anal. found/calcd.: C, 40.6/40.9; H, 2.5/2.7 % for **1**. IR (KBr, cm⁻¹): 3508(m), 3045(w), 2969(w), 1957(w), 1609(s), 1564(m), 1395(s), 1297(m), 1163(m), 1011(w), 838(w), 784(w), 731(s), 619(m), 432(w).

Microwave Synthesis of $[\text{Mg}_3(\text{OH})_2(\text{SBA})_2(\text{EtOH})(\text{H}_2\text{O})_3]\cdot 3.5\text{H}_2\text{O}$ (2). A mixture of H_2SBA (0.1224 g, 0.4 mmol), $\text{Mg}(\text{NO}_3)_2\cdot 6\text{H}_2\text{O}$ (0.4100 g, 1.6 mmol), EtOH (5.0 mL) and H_2O (1.0 mL) was heated at 150 °C for 20 min. The colorless crystals of **2** were filtered off, washed with EtOH, dried in room temperature atmosphere, and collected with the yield of 0.0720 g (41.21 %, based on the H_2SBA reagent). Anal. found/calcd.: C, 41.77/41.00; H, 3.99/4.24 % for **2**. IR (KBr, cm^{-1}): 3531(w), 3268(w), 2978(w), 1620(s), 1564(m), 1413(s), 1291(m), 1165(m), 1102(m), 789(w), 746(s), 698(w), 621(w), 491(w), 442(w).

Microwave Synthesis of $[\text{Ni}_3(\text{OH})_2(\text{SBA})_2(\text{EtOH})(\text{H}_2\text{O})_3]\cdot 3.5\text{H}_2\text{O}$ (3) The compound **3** was obtained from a reaction mixture of H_2SBA (0.0612 g, 0.2 mmol), $\text{NiCl}_2\cdot 6\text{H}_2\text{O}$ (0.0475 g, 0.2 mmol), DMF (3.0 mL), (EtOH, 7.0 mL), and H_2O (1.0 mL). The mixture was heated at 180 °C for 20 min. The green crystals of **3** were filtered off, washed with EtOH, dried in room temperature atmosphere, and collected with the yield of 0.0425 g (43.41 %, based on the H_2SBA reagent). Anal. found/calcd.: C, 36.92/36.84; H, 3.48/3.53 % for **3**. IR (KBr, cm^{-1}): 3525(m), 3226(b), 1680(s), 1608(s), 1569(s), 1482(s), 1285(s), 1156(s), 1104(s), 1011(s), 743(s), 684(s), 628(s), 490(s), 422(s).

Microwave Synthesis of $[\text{Co}_3(\text{OH})_2(\text{SBA})_2(\text{EtOH})(\text{H}_2\text{O})_3]\cdot 3.5\text{H}_2\text{O}$ (4) The compound **4** was obtained from a reaction mixture of H_2SBA (0.0612 g, 0.2 mmol), $\text{CoCl}_2\cdot 6\text{H}_2\text{O}$ (0.0475 g, 0.2 mmol), DMF (3.0 mL), EtOH (7.0 mL), and H_2O (1.0 mL). The mixture was heated at 150 °C for 20 min. The pink crystals of **4** were filtered off, washed with EtOH, dried in room temperature atmosphere, and collected with the yield of 0.0503 g (51.23 %, based on the H_2SBA reagent). Anal. found/calcd.: C, 36.79/36.67; H, 3.82/3.80 % for **4**. IR (KBr, cm^{-1}): 3529(m), 3224(b), 1682(s), 1601(s), 1572(s), 1480(s), 1159(s), 1101(s), 741(s), 624(s), 493(s), 425(s).

Microwave Synthesis of $[\text{Mn}(\text{SBA})(\text{EtOH})]$ (5). The compound **5** was obtained from a reaction mixture of H_2SBA (0.1224 g, 0.4 mmol), $\text{Mn}(\text{NO}_3)_2\cdot 4\text{H}_2\text{O}$ (0.2000 g, 0.8 mmol), EtOH (5.0 mL) and H_2O (1.0 mL). The mixture was heated at 180 °C for 20 min. Only very few light-pink crystals of **5** were collected.

Microwave Synthesis of $[\text{Mn}(\text{SBA})(\text{H}_2\text{O})]$ (6). The compound **6** was obtained from a reaction mixture of H_2SBA (0.2448 g, 0.8 mmol), $\text{Mn}(\text{NO}_3)_2\cdot 4\text{H}_2\text{O}$ (0.2000 g, 0.8 mmol), EtOH (7.0 mL), and H_2O (3.0 mL). The mixture was heated at 180 °C for 20 min. Only very few colorless crystals of **6** were collected.

Preparation of de-solvated phases, $[\text{M}_3(\text{OH})_2(\text{SBA})_2]$ (CYCU-5 and 2a-4a). The heating of as-synthesized compounds **1-4** at 200 °C for 10 h resulted the de-solvated phases (CYCU-5 and 2a-4a).

Single-Crystal Structure Analysis

The diffraction measurements were performed on Bruker AXS SMART APEX II diffractometer (Mo-K α radiation, graphite monochromator, $\lambda = 0.71073 \text{ \AA}$). All data were corrected for Lorentz and polarization effects, and the program *SADABS* in *APEX2*¹⁵ was used for the absorption correction. On the basis of systematic absences and statistics of intensity distribution, all the single crystal structures were solved with metal atoms being disclosed first, followed by the atoms of O, N, and C located on successive difference Fourier maps. The H atoms were added in idealized positions and constrained to ride on their parent atoms. All calculations were performed by using *SHELXTL* programs in *APEX2*.¹⁶ While the framework structure of **1** was refined easily, the solvent molecules in **1** could not be refined because of their highly disordered structure. Therefore, SQUEEZE function of the PLATON program was used to eliminate the contribution of the electron density in the solvent region from the intensity data. Crystallographic data are given in Table 1. Selected bond lengths are listed in Table S1 (Supporting Information). Crystallographic data (CIF) for the single crystal structure reported in this paper have been deposited with the Cambridge Crystallographic Data Centre (CCDC) as supplementary publication numbers CCDC-943771, 943772, 805748, 998723, and 998724 for the compounds, **1**, **CYCU-5**, **2**, **5**, and **6** respectively.

Table 1. Single Crystal Crystallographic Data.

	1	CYCU-5	2	5	6
formula	C ₁₅ H ₁₂ Zn _{1.5} O _{7.5} S	C ₁₄ H ₉ Zn _{1.5} O ₇ S	C ₃₀ H ₃₇ Mg ₃ O _{21.5} S ₂	C ₁₆ H ₁₃ MnO ₇ S	C ₁₄ H ₁₀ MnO ₇ S
fw	442.36	419.33	878.65	404.26	377.22
space group	<i>P2₁/n</i>	<i>P2₁/n</i>	<i>P2/c</i>	<i>P2₁/n</i>	<i>P-1</i>
<i>a</i> (Å)	14.0847(4)	14.1168(2)	28.1637(9)	10.1610(5)	5.998(2)
<i>b</i> (Å)	5.9953(2)	6.0531(10)	6.441(2)	7.3197(3)	11.8959(4)
<i>c</i> (Å)	19.3347(6)	19.3678(3)	24.8679(8)	22.3295(10)	13.0287(7)
α (°)	90	90	90	90	112.118(3)
β (°)	93.729(2)	93.627(10)	115.445(2)	93.6990(10)	102.502(3)
γ (°)	90	90	90	90	99.816(2)
<i>V</i> (Å ³)	1629.20(9)	1651.67(4)	4073.6(2)	1657.31(13)	807.49(6)
<i>Z</i>	4	4	4	4	2
<i>D</i> _{calc} (gcm ⁻³)	1.803	1.686	1.433	1.620	1.551
μ (mm ⁻¹)	2.393	2.353	0.28	0.959	0.978
Reflections collected	26234	15157	45162	14612	13815
Independent reflections	4029	4098	10210	4090	3960
R(int)	0.0337	0.0300	0.0806	0.0381	0.0344
Goodness-of-fit on F ²	1.147	0.979	1.037	1.165	1.082
R1 [<i>I</i> >2 σ (<i>I</i>)]	0.0459	0.0301	0.0541	0.0572	0.0492
wR2 [<i>I</i> >2 σ (<i>I</i>)]	0.1146	0.0709	0.1468	0.1548	0.1241
R1 [all data]	0.0508	0.0470	0.1118	0.0630	0.0601
wR2(all data)	0.1167	0.0785	0.1672	0.1573	0.1282
CCDC No.	943771	943772	805748	998723	998724

Structural Matching and Powder X-Ray Diffraction (PXRD) Analysis

The powder X-ray diffraction (PXRD) patterns were also recorded at the BL01C2 beamline of the National Synchrotron Radiation Research Center (NSRRC) in Taiwan. The ring energy of NSRRC was operated at 12 keV with a typical current of 300 mA. The wavelength of the incident X-rays was 1.0332 Å, delivered from the superconducting wavelength-shifting magnet, and a Si(111) double-crystal monochromator. The diffraction patterns were recorded with a Mar345 imaging plate detector approximately 280 mm from sample positions and typical exposure duration of 5 min. The pixel size of Mar345 was 100 μm. The one-dimensional powder diffraction profile was converted with program FIT2D and cake-type integration. The diffraction angles were calibrated according to Bragg positions of Ag-Benhenate and Si powder (NBS640b) standards. The powder sample was sealed in a capillary (0.7 mm diameter) and heated in a stream of hot air. The Rietveld refinements of all powder samples were carried out with the GSAS program.¹⁷ Crystallographic details of the compounds determined from synchrotron PXRD data are given in Table 2&3 and Table S4 (Supporting Information). Selected bond lengths are listed in Table S5&S6 (Supporting Information). The Rietveld plot corresponds to the crystal structure model and profile factors are displayed in Figure S7&S8 (Supporting Information). Crystallographic data (CIF) for the powder samples structural refinements were published as Supplementary information.

Table 2. Crystallographic details of **3** and **4** at 303K, as determined from synchrotron PXRD data.

	3 (83%)	3a (17%)	4
Chemical formula	C ₃₀ H ₂₉ Ni ₃ O ₁₈ S ₂	C ₂₈ H ₁₈ Ni ₃ O ₁₄ S ₂	C ₃₀ H ₂₉ Co ₃ O ₁₈ S ₂
Formula weight	914.89	815.8	917.88
Crystal system	Monoclinic	Monoclinic	Monoclinic
Temperature (K)	303	303	303
Space group	<i>P2/c</i>	<i>P2₁/n</i>	<i>P2/c</i>
<i>a</i> (Å)	27.051(7)	12.738(6)	28.1888(19)
<i>b</i> (Å)	6.2522(14)	6.240(6)	6.3545(3)
<i>c</i> (Å)	24.945(8)	21.545(8)	24.9584(15)
β (°)	115.191(12)	89.61(5)	115.737(4)
<i>V</i> (Å ³)	3817.66(183)	1712.47(219)	4027.2(4)
<i>Z</i>	4	2	4
Radiation (Å)	1.0332	1.0332	1.0332
χ^2	6.332	6.332	2.346
<i>R_p</i> (%)	5.31	5.31	4.64
<i>R_{wp}</i> (%)	7.53	7.53	7.08

Table 3. Crystallographic details of CYCU-5, **2a-4a** at 473K, as determined from synchrotron PXRD data.

	CYCU-5	2a	3a	4a
Chemical formula	C ₂₈ H ₁₈ Zn ₃ O ₁₄ S ₂	C ₂₈ H ₁₈ Mg ₃ O ₁₄ S ₂	C ₂₈ H ₁₈ Ni ₃ O ₁₄ S ₂	C ₂₈ H ₁₈ Co ₃ O ₁₄ S ₂
Formula weight	833.8	714.0	815.8	818.8
Crystal system	Monoclinic	Monoclinic	Monoclinic	Monoclinic
Temperature (K)	473	473	473	473
Space group	<i>P2₁/n</i>	<i>P2₁/n</i>	<i>P2₁/n</i>	<i>P2₁/n</i>
<i>a</i> (Å)	13.9323(6)	14.307(21)	13.9069(32)	13.881(14)
<i>b</i> (Å)	6.0385(2)	6.082(5)	6.1607(10)	6.1930(26)
<i>c</i> (Å)	19.3839(8)	18.816(17)	19.288(7)	20.006(13)
β (°)	93.2021(22)	89.325(11)	90.30(4)	90.0(1)
<i>V</i> (Å ³)	1628.3(2)	1637.16(313)	1652.5(8)	1719.82(219)
<i>Z</i>	2	2	2	2
Radiation (Å)	1.0332	1.0332	1.0332	1.0332
χ^2	2.653	3.425	6.479	4.447
<i>R_p</i> (%)	2.49	6.74	5.55	6.818
<i>R_{wp}</i> (%)	4.54	9.90	9.03	9.90

Results and Discussion

Structural Description of [Zn₃(OH)₂(SBA)₂] \cdot EtOH (1** or CYCU-5 \cdot EtOH).** Single crystal X-ray diffraction structure analysis shows that the structure of the compound **1** possesses an extended 2D framework. The asymmetric unit consists of two crystallographically independent Zn centers and two SBA ligand units (Figure 1a). The Zn(1) center is six-coordinated and bonded to four oxygen atoms of the carboxylate groups belonging to four SBA units, and the remaining two octahedral coordination sites which are ‘*trans*’ to each other, have been occupied by two oxygen atoms (O3) of the two hydroxide ions. On the other hand, the tetrahedrally four-coordinated Zn(2) atom is coordinated with two oxygen atoms of the carboxylate groups belonging to two SBA ligand units, and two oxygen atoms (O3) of the two hydroxide ions. The hydroxide ions act as bridge to connect the Zn(1) and Zn(2) centers. The SBA ligand is tetradentate, which is bridging to four Zn centers through each of its four carboxylate oxygen atoms (Figure 1b). All of the Zn-O bonds distances range from 1.909(3) to 2.170(3) Å (Table S1, Supporting Information). As shown in Figure 1c, the inorganic motif displays a 1D chains were formed by the edge-sharing Zn₂O₁₀ and corner-sharing ZnO₆. The one dimensional inorganic building unit in compound **1** has been reported previously for a zinc terephthalate open framework.¹⁸ These chains are linked together by the μ_4 -links of SBA ligands in two directions to generate the 2D metal-organic framework of **1** (Figure 1d). The layers are further interacted by hydrogen bonds (Table S2, Supporting Information). The framework contains rhomboidal-channels with a free diameter of 5.1 x 4.7 Å² (considering the van der Waals radii of

atoms) without including the water and EtOH molecules. The solvent accessible volume (SAV) calculated without including ethanol and water molecules by PLATON¹⁹ analysis is 301.7 Å³ which is 18.5 % of the unit cell volume.

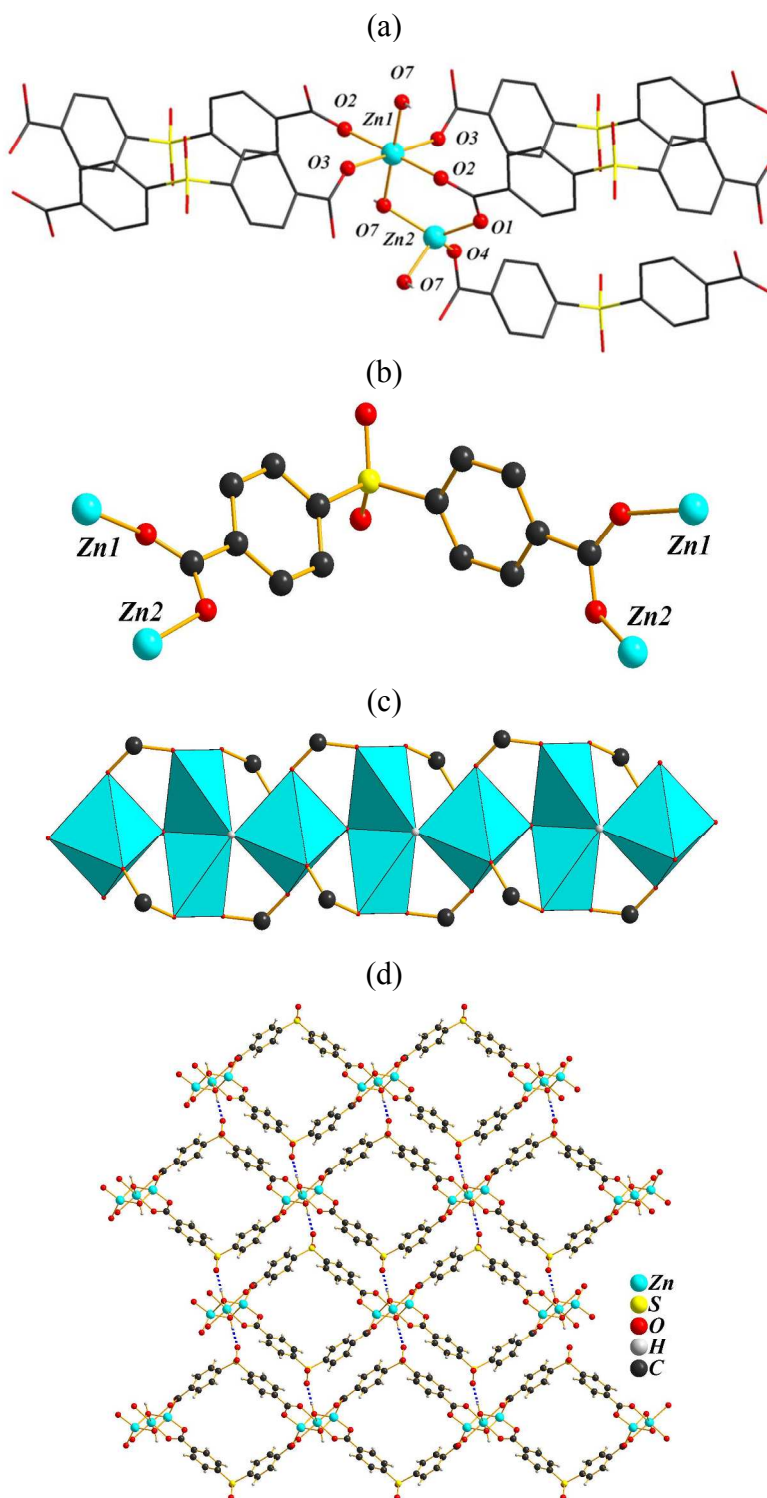
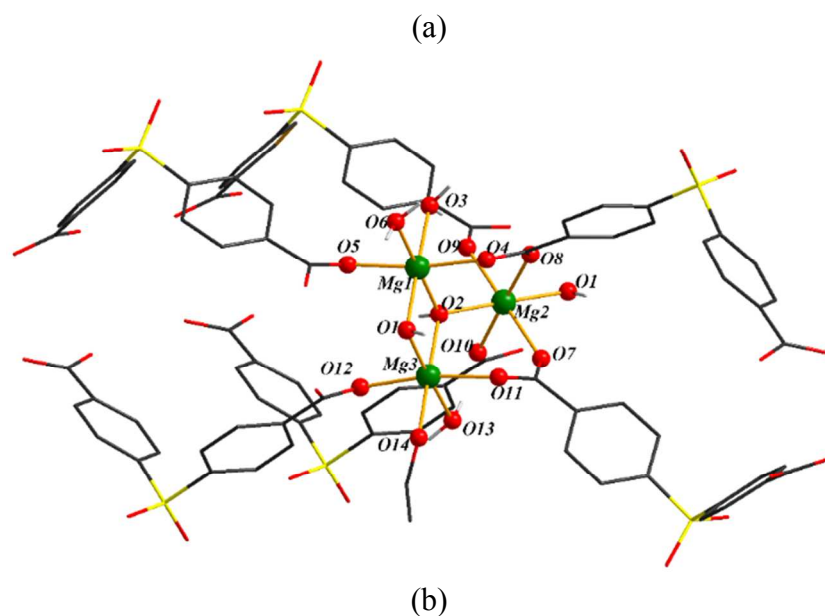


Figure 1. (a) The coordination spheres of Zinc atoms in **1**. (b) The coordination environment of SBA ligand. (c) The edged-sharing and cornered-sharing 1D inorganic chain in **1**. (d) The 2D structure view of **1** with the channels along *b*-axis.

Structural description of $[\text{M}_3(\text{OH})_2(\text{SBA})_2(\text{EtOH})(\text{H}_2\text{O})_3] \cdot 3.5\text{H}_2\text{O}$ (2-4, M=Mg, Ni, Co).

Single crystal X-ray structure analysis of compounds **2** and PXRD fitting of compounds **3** and **4** displayed that compounds **2** to **4** have the similar conformations of $[\text{Co}_3(\text{OH})_2(\text{SBA})_2(\text{EtOH})(\text{H}_2\text{O})_3] \cdot 3.5\text{H}_2\text{O}$ ¹³ which was synthesized by conventional heating. For **2**, all of the Mg-O bonds distances range from 2.049(2) to 2.124(2) Å (Figure 2a, Table S1, Supporting Information). The layer structure of **2** (Figure 2b) consists of $[\text{Mg}_3(\mu_3\text{-OH})_2]_n$ chains linked by SBA ligands. In the chain, the Mg atoms, Mg(1), Mg(2) and Mg(3), are first linked by one $\mu_3\text{-OH}$. Along the chain direction (*b*-axis) these three magnesium centers are further connected by another $\mu_3\text{-OH}$. Within the 1D chains, the Mg(2)O₆ and Mg(3)O₆ octahedra are edge-sharing, and they are apex-shared with the Mg(1)O₆ octahedra (Figure 2c). The layers are further connected by hydrogen bonds between the coordinated water molecules and oxygen atoms on sulfone group (Table S2, Supporting Information). Each layer contains rhomboidal-channels with a free diameter of 5.2 x 4.7 Å² (considering the van der Waals radii of atoms) without including the water and EtOH molecules. The SAV calculated without including ethanol and water molecules by PLATON¹⁹ analysis is 1319.4 Å³ which is 32.4% of the unit cell volume. The comparison of this hypothetical calculation with the results of CYCU-5 clearly indicates that, if the solvent molecules of **2** removed without structural transformation or distortion leads to larger free pore volume.



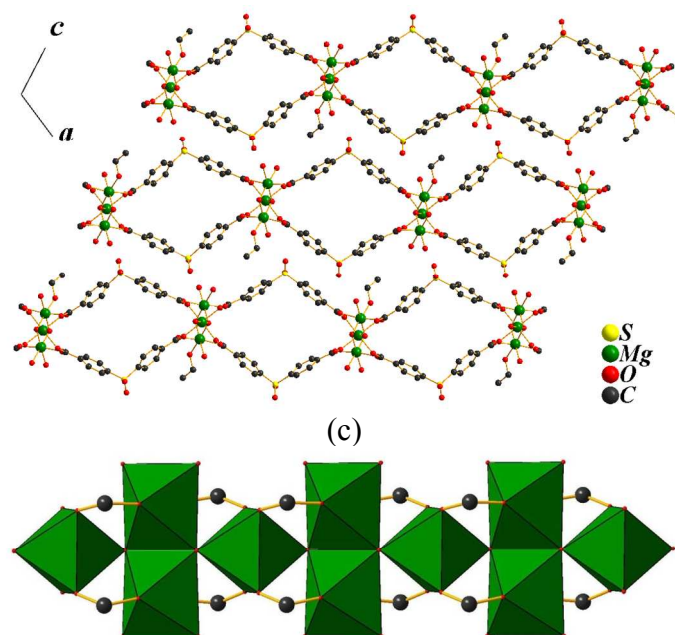


Figure 2. (a) The coordination spheres of magnesium atom in **2**. (b) The 2D structure view of **2** with the channels along *b*-axis. (c) The edged-sharing and cornered-sharing 1-D inorganic chain in **2**.

Structural description of [Mn(SBA)(EtOH)] (5). Single crystal structure analysis shows that the structure of the compound **5** also possesses an extended 2D framework. The asymmetric unit consists of one crystallographically independent Mn center, one SBA ligand, and one EtOH (Figure 3a). The Mn(II) ion is six-coordinated and bonded with five oxygen atoms from the carboxylate groups belonging to four SBA ligands, and one oxygen atom from the coordinated EtOH molecule. The SBA ligand has acted as pentadentate and coordinated with four Mn centers (Figure 3b) through its carboxylate oxygen atoms. The Mn-O bonds distances range from 2.085(3) to 2.369(3) Å (Table S1, Supporting Information). As shown in Figure 3c, the inorganic motif displays a 1D chains were formed by the corner-sharing MnO_6 polyhedra. These chains are linked together by the SBA ligands in two directions to generate the 2D metal-organic framework of **5** (Figure 3d). The framework of **5** contains rhomboidal-channels with a free diameter of $5.9 \times 5.3 \text{ \AA}^2$ (considering the van der Waals radii of atoms) without including the water and EtOH molecules. The SAV calculated without including ethanol molecules by PLATON¹⁹ analysis is 374.2 \AA^3 which is 22.6 % of the unit cell volume. This value is comparable to that of **CYCU-5**.

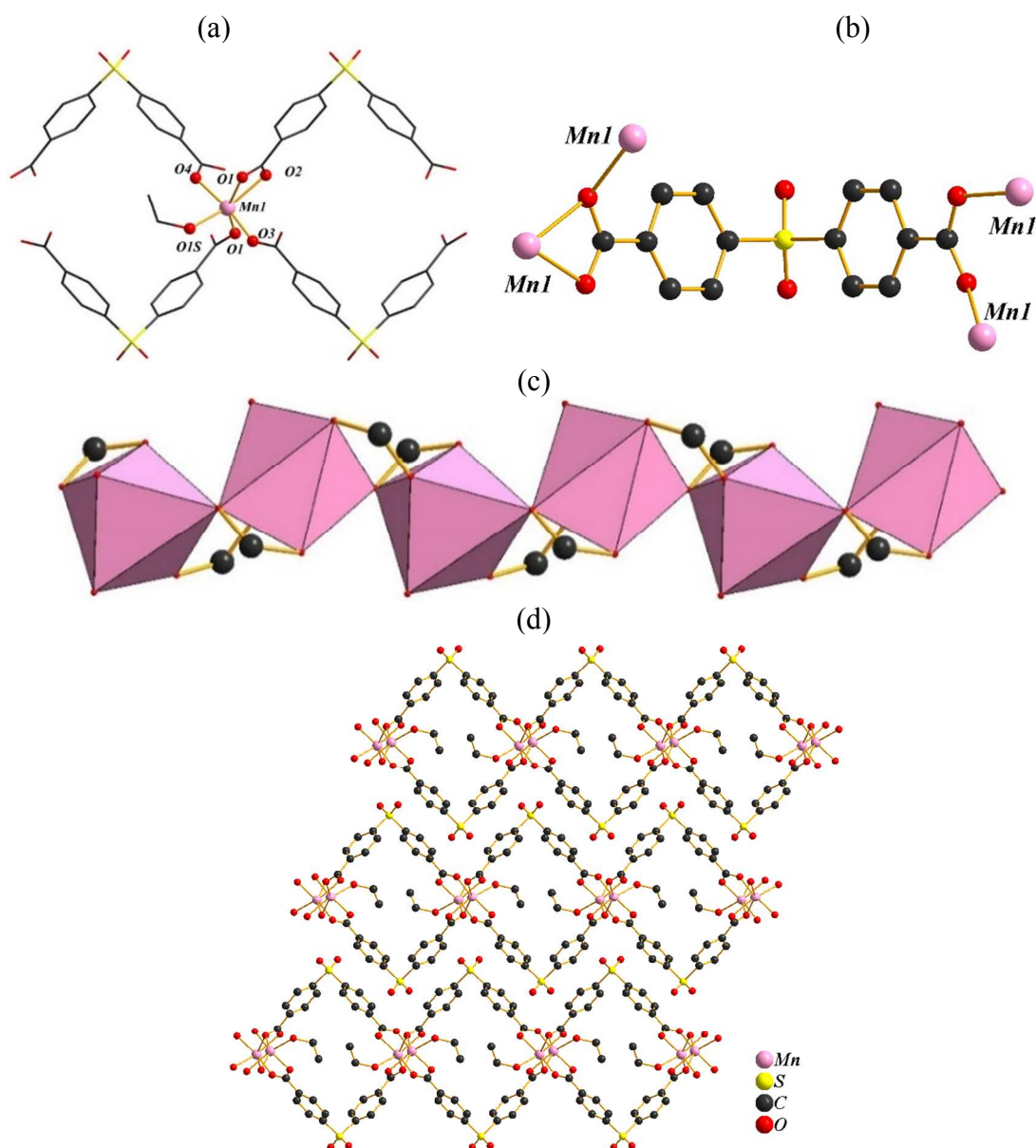


Figure 3. (a) The coordination spheres of Mn in **5**. (b) The coordination environment of SBA ligand in **5**. (c) The edged-sharing 1D inorganic chain in **5**. (d) The 2D structure view of **5** with the channels along *b*-axis.

Structural description of [Mn(SBA)(H₂O)] (6). Single crystal X-ray diffraction shows that the structure of the compound **6** also possesses an extended 2D framework. The asymmetric unit consists of one independent Mn center, one SBA ligand, and one coordinated water molecule (Figure 4a). The Mn(II) ion is six-coordinated and binds with six oxygen atoms from the carboxylate groups belonging to five H₂SBA ligands, and one oxygen atom from the coordinated water molecule. The H₂SBA ligand overall is pentadentate bridging with five Mn(II) ions through each of its five carboxylate oxygen atoms (Figure 4b). The Mn-O bond distances range from 2.126(2) to 2.284(2) Å (Table S1, Supporting Information). As shown in Figure 4c, the inorganic motif displays a 1D chains

which were formed by the edged-sharing Mn_2O_{10} that are connected by SBA ligand units. These chains are further linked together by the μ_5 -links of SBA ligands in two directions to generate the 2D metal-organic framework of **6** (Figure 4d). The framework contains rhomboidal-channels with a free diameter of $5.6 \times 5.0 \text{ \AA}^2$ (considering the van der Waals radii of atoms) without including the water molecules. The SAV calculated without including water molecules by PLATON¹⁹ analysis is 129.6 \AA^3 which is 16.1% of the unit cell volume. The less number of coordinated solvent molecules in structure reduce the possible free volume in compound **6**.

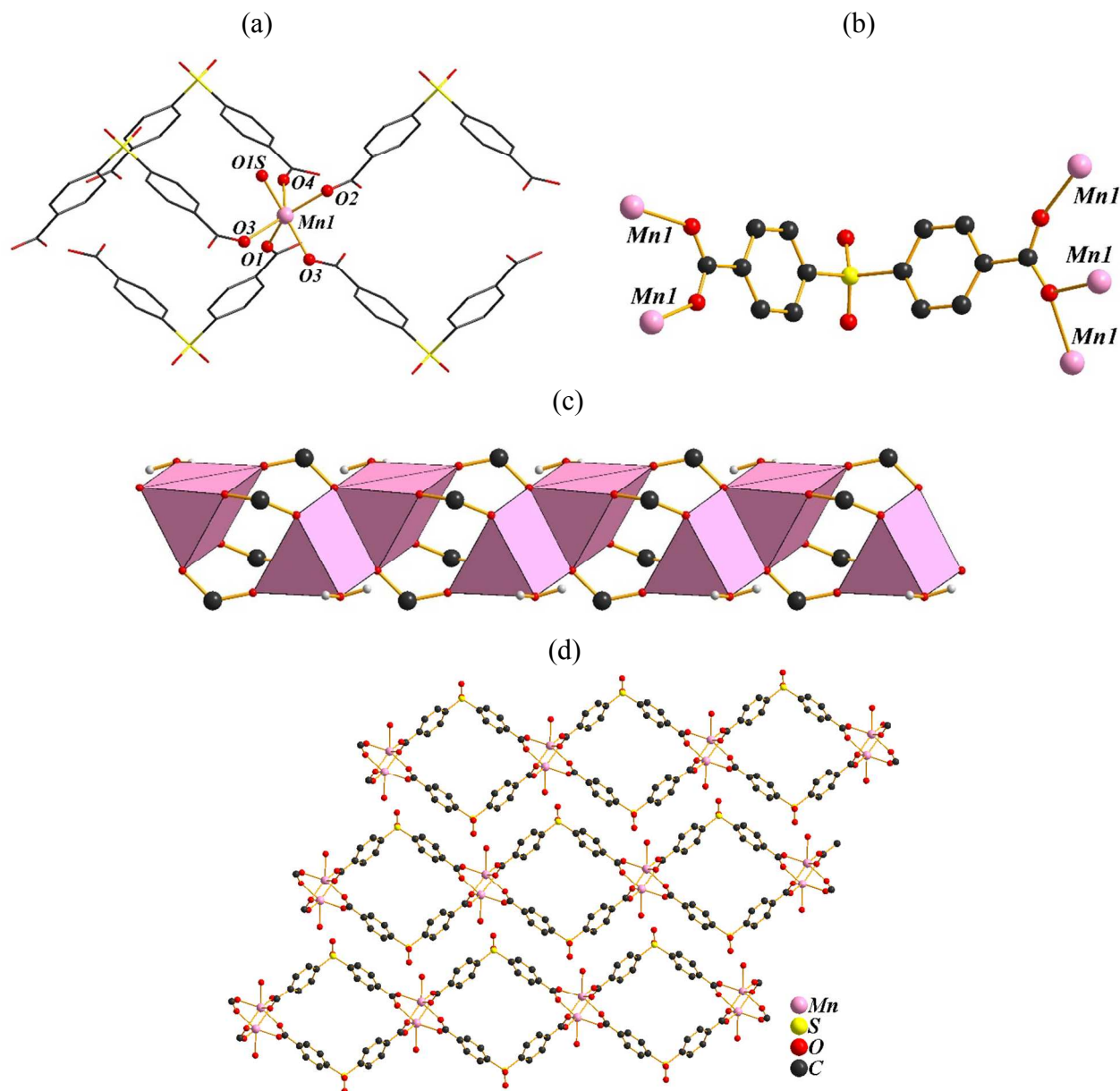


Figure 4. (a) The coordination spheres of Mn atom in **6**. (b) The coordination environment of SBA ligand in **6**. (c) The edged-sharing and cornered-sharing 1D inorganic chain in **6**. (d) The 2D structure view of **6** with the channels along b -axis.

Evaluation of Structural Transformation

It is interesting to note that the various temperature PXRD patterns of **1** displayed similar pattern up to 673 K (Figure S2, Supporting Information) which indicates the SBUs of inorganic chains are remains stable with ZnO_4 tetrahedra and ZnO_6 octahedra under high temperature (673 K). All these PXRD patterns were evaluated in detail by carrying out Rietveld profile fitting (Figure 5 and Figure S7, Supporting Information) which displayed that the lattice parameters change upon activation (Figure 6). The results showed increasing trend for lattice parameters along a - and b -axis as temperature increases, while the c -axis showed decreasing trend after 423 K. The unit cell volume generally expand when the temperature was added. As shown in Table S6 (Supporting Information), two type of bond length (Zn2-O2 and S1-O4) and one distance ($\text{O1}\cdots\text{O4}$) are consisted with the variation of c -axis. Both tetrahedral distortion and hydrogen bonding could fit well to contribute the structural transformation.

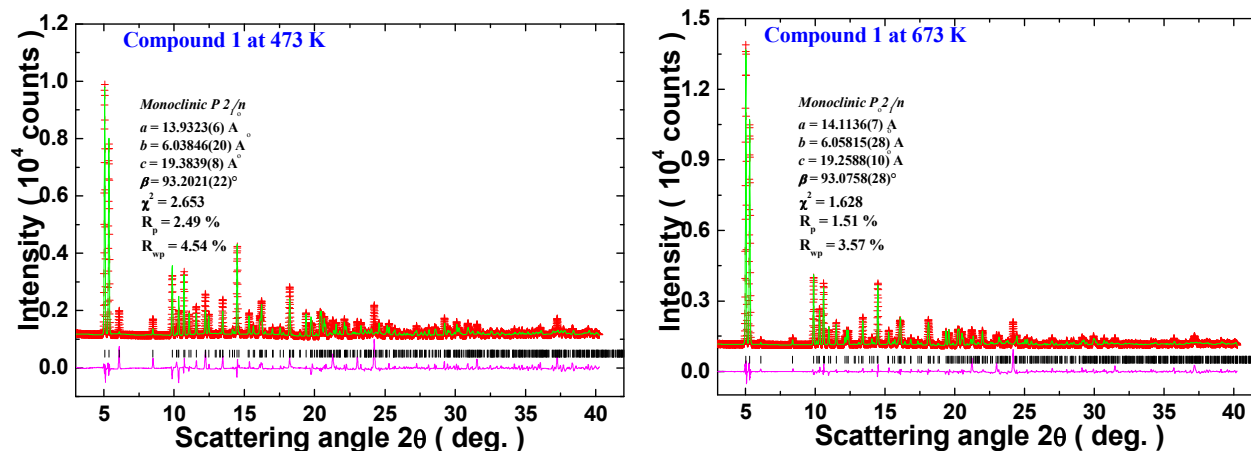
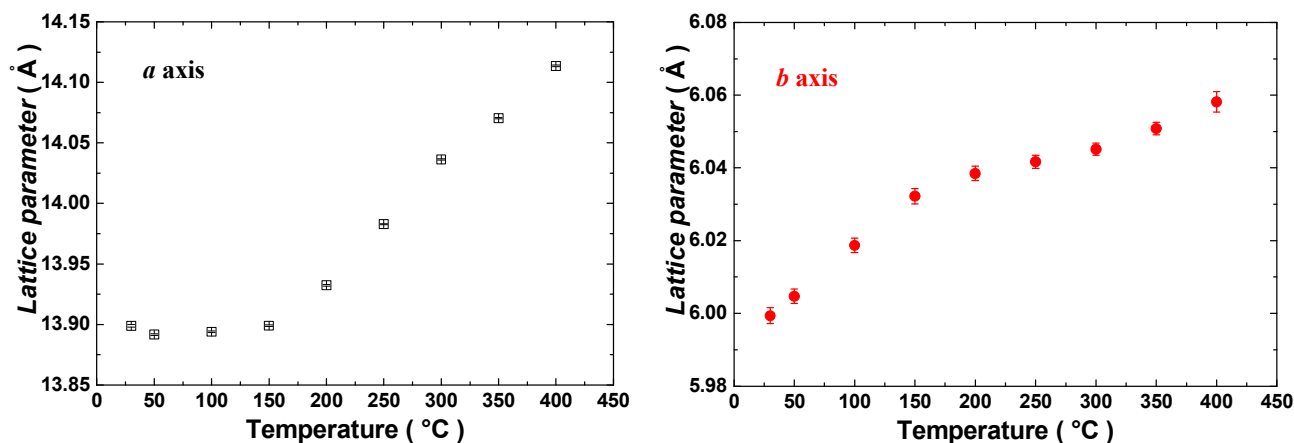


Figure 5. Rietveld profile fits to synchrotron PXRD data for CYCU-5 at 473 K and 673 K. The measured values are in red, the calculated intensity is in green and the difference plot is in pink color.



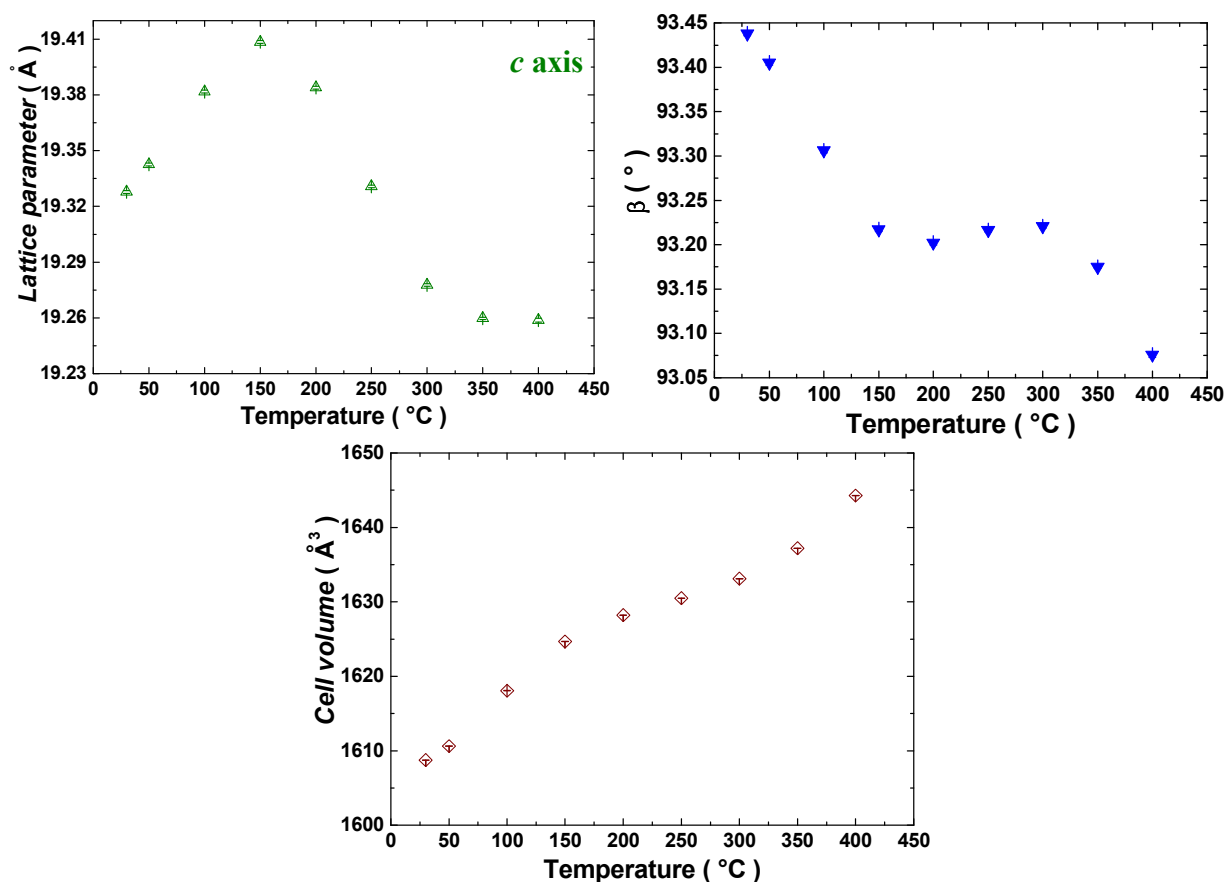


Figure 6. Final Rietveld refinements lattice parameters for **1** at various temperature.

All de-solvated samples of **2a-4a** are isostructural and that the same structure as in activated **1** with monoclinic crystal system and $P2_1/n$ space group (Figure 7). In **2-4**, the first two peaks in the PXRD pattern transfer to **2a-4a** with one main peak at 473 K which may be corresponding to the solvent removal and the structural transformation to **CYCU-5** like frameworks (Figure S3-S5, Supporting Information). However, few extra phase (intermediate phase) in varied temperature PXRD patterns of **3** at 303-473 K and **4** at 373 K have been observed (Figure S4&S5, Supporting Information) which were structurally identified as as-synthesized and de-solvated phases. The Rietveld profile fits to synchrotron PXRD data for **3** and **4** showed that the percentage ratio of as-synthesized and de-solvated phases are 83/17 and 67/33 respectively. For **2a-4a**, as shown in Table S7 (Supporting Information), the bond length (M2–O2) relative to tetrahedral distortion and both bond length (S1–O4) and distance (O1···O4) relative to hydrogen bonding are the main considerations during the structural transformation. Finally, the PXRD pattern of **CYCU-5** and **2a-4a** at 473 K were well fitted and of reveals that the activation frameworks should have similar conformation.

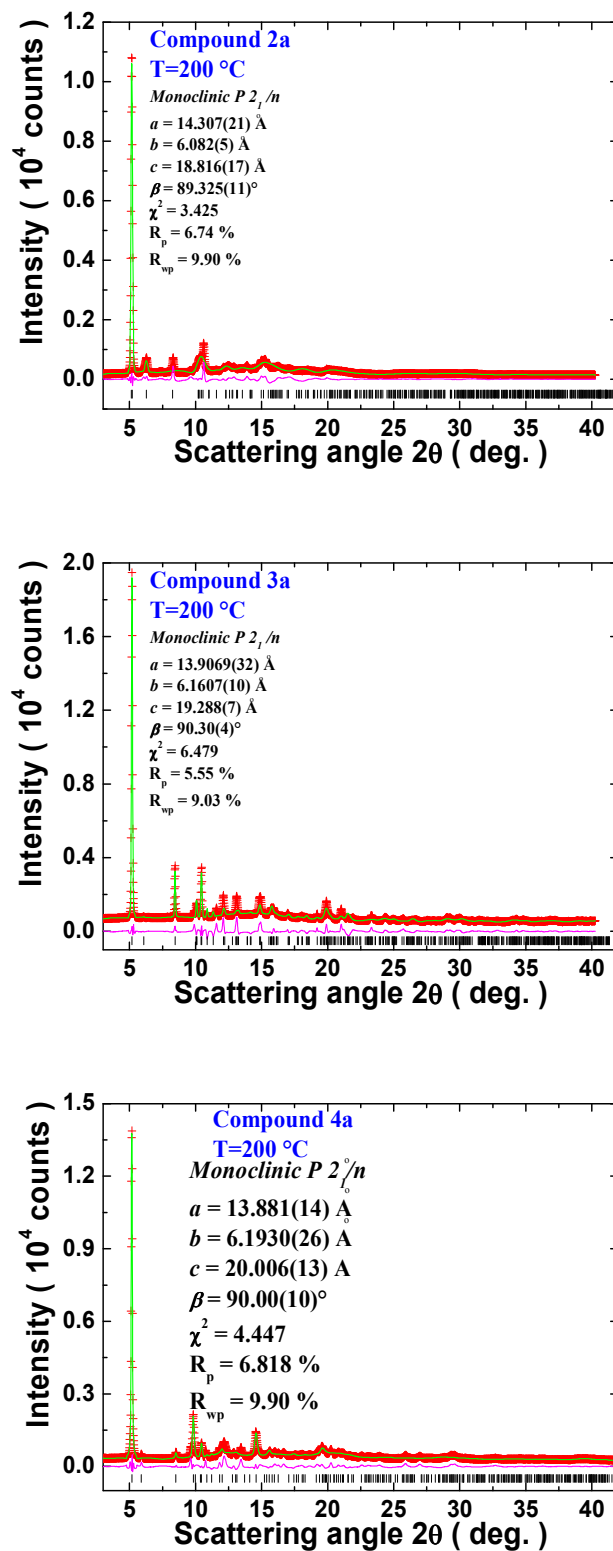


Figure 7. Final Rietveld-plot for **2a** to **4a** at 473 K. The measured values are in red, the calculated intensity is in green and the difference plot is in pink color.

Thermogravimetry Analysis

Thermogravimetry analyses (TGA) were performed to determine the thermal stability of the studied compounds **1-4** (Figure S1, Supporting information) and their corresponding weight losses of solvent molecules at the different temperatures with their calculated weight losses are tabulated (Table S3, Supporting information). TGA curve of **1** showed the gradual first weight loss of about 6% up to 300 °C is corresponding to the release of crystalized ethanol molecule (*ca.* 5.2%). So, the **CYCU-5** was thermally stable up to about 400 °C. The further weight loss till to 800 °C, might be corresponding to the decomposition of organic ligands which formed zinc oxide (Figure S7, Supporting Information). The TGA curve of **2** revealed that all the water and ethanol molecules are easily removed in two steps slightly above 150 °C, and the mass loss of 18.1% agrees well with the calculated 16.8%; it might lose its lattice water molecules in the first step, followed by the loss of coordinated water and ethanol molecules in the second step. Further, the desolvated phase, $[\text{Mg}_3(\text{OH})_2(\text{SBA})_2]$ was fairly stable up to 400 °C, then the framework of **2** was started to decompose. Whereas, the TGA curves of compounds **3** and **4** have showed similar thermal stability behavior as we seen in **2**. That is, the water and ethanol molecules removal has been occurred in two steps at around 200 °C and 120 °C for the compounds **3** and **4** respectively. It is noteworthy to mention that the desolvated phase of **3** and **4** are thermally stable up to 350 °C. Further heating of the compounds up to 800 °C results in decomposition of framework structures. As displayed in Figure S8 (Supporting Information), the Rietveld profile fits to synchrotron PXRD data for **4** at 673 K has showed the existence of three types of cobalt oxides.

Gas Sorption Properties

To verify the porosity of guest free phase of the compounds **1-4** (**CYCU-5**, **2a**, **3a**, and **4a**), gas sorption isotherms have been measured with N_2 , CO_2 and H_2 . The N_2 gas adsorption isotherm at 77 K for the compounds shows type-I behavior with a steep rise in the very low pressure region, suggesting a microporous nature. The N_2 gas sorption results of compounds **CYCU-5**, **2a**, **3a**, and **4a** are tabulated in Table 4. From the results obtained from the N_2 gas sorption experiments (Figure 8), it has been found that compound **4a** has better N_2 gas sorption capacity than that of the rest of the three (**CYCU-5**, **2a** and **3a**).

Table 4 The N_2 gas sorption data of **CYCU-5**, **2a**, **3a** and **4a**.

Compound	BET Surface Area (m^2/g)	Langmuir Surface Area (m^2/g)
CYCU-5	19.6	24.1
2a	44.5	59.9

3a	9.7	11.7
4a	71.5	92.6

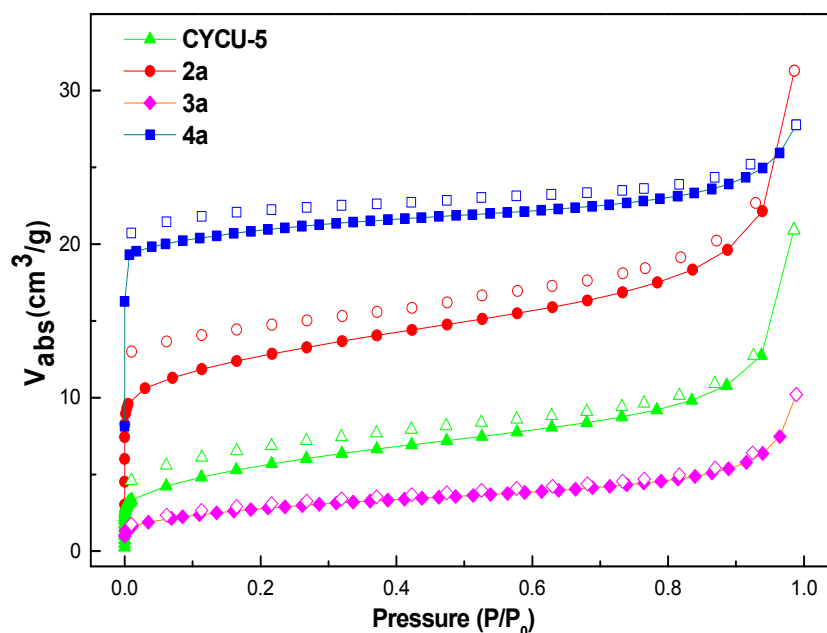


Figure 8. Nitrogen adsorption isotherms for the compounds, CYCU-5, 2a, 3a and 4a.

In the case of CO₂ adsorption isotherm for the compounds at 273 and 298 K (Figure 9), the compounds showed moderate CO₂ adsorption behavior and their corresponding values are depicted in Table 5. All the compounds showed better CO₂ uptake at low temperature (273 K) than the room temperature (298 K). The compound 4a showed highest CO₂ gas sorption behavior among the four as we have seen in the N₂ case also. The results of CO₂ uptake for the compounds are comparable with some of the reported compounds, Zn₂(tetrakis[4-(carboxyphenyl)oxamethyl]methane)(4,4'-bipyridine),²⁰ and MOF-5/IRMOF-1²¹ under similar conditions.

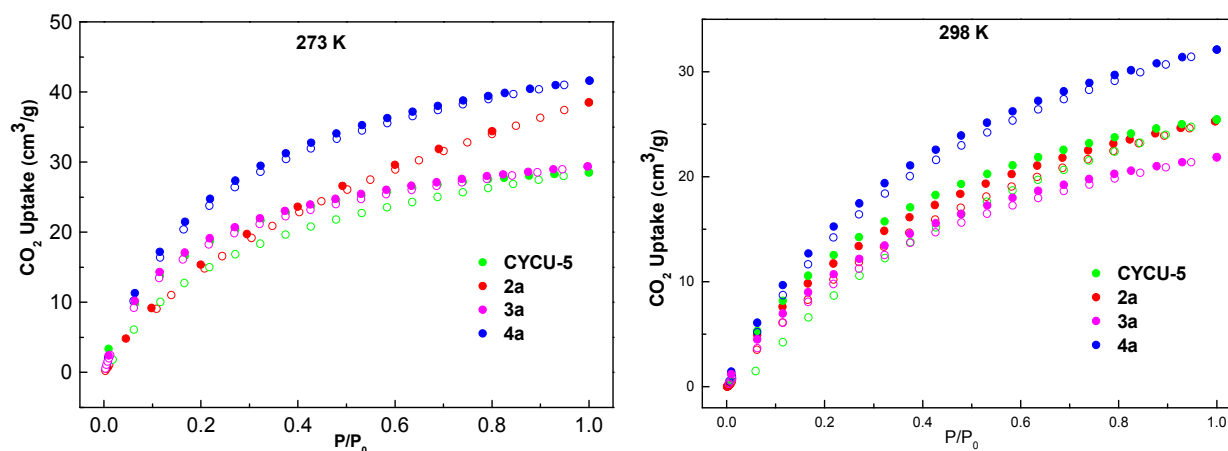
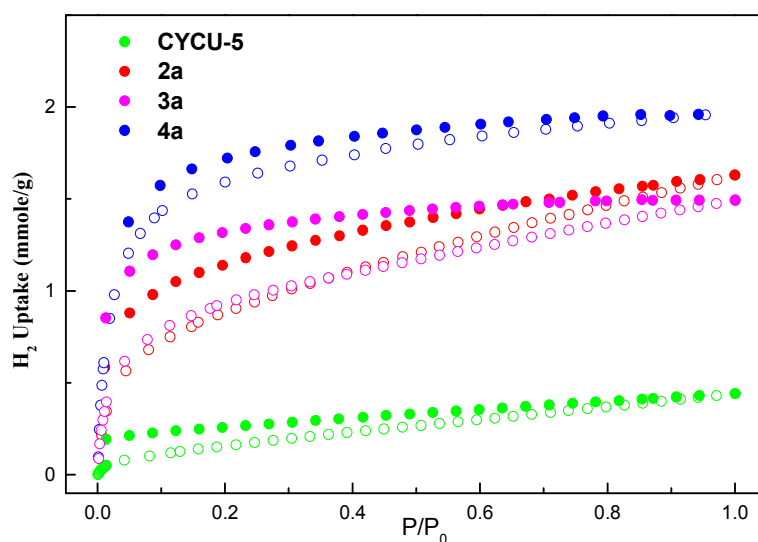


Figure 9. The CO₂ adsorption isotherms for the compounds, CYCU-5, 2a, 3a and 4a, measured at 273 K and 298 K.

Table 5 The CO₂ and H₂ uptake data of **CYCU-5**, **2a**, **3a** and **4a**.

Compounds	CO ₂ Uptake in cm ³ /g (mmol/g) at 1 atm		H ₂ Uptake at 77 K, 1 atm in mmol/g (wt%)
	273 K	298 K	
CYCU-5	29.39 (1.31)	21.87 (0.98)	0.44 (0.09)
2a	38.52 (1.72)	25.28 (1.13)	1.63 (0.32)
3a	28.54 (1.27)	25.46 (1.14)	1.49 (0.30)
4a	41.62 (1.86)	32.11 (1.43)	1.96 (0.39)

On the other hand, The H₂ gas sorption properties of the compounds have been studied at 77 K (Figure 10). All the four compounds showed some amount of H₂ uptake at 1 atm which are given in Table 5. Like in the previous two cases, the compound **4a** exhibited better H₂ storage capacity among the four compounds studied. Surprisingly, **CYCU-5** displayed almost no H₂ gas sorption property. The H₂ gas sorption capacity of **4a**, **3a** and **2a** are comparable with the reported compounds, [Cu(hfipbb)(h₂hfipbb)_{0.5}],²² PCN-13,²³ [Mn(NDC)],²⁴ and [Cd₂(Tzc)₂]²⁵ under similar conditions.

**Figure 10.** The H₂ adsorption-desorption isotherms of **CYCU-5**, **2a**, **3a** and **4a**, at 77 K.

In order to explore the potential gas separation properties of **CYCU-5** under ambient conditions, the adsorption isotherms of CO₂, N₂, and CH₄ for **CYCU-5** at 273 K were measured (Figure 11). The CO₂ uptake value at 1 atm is 5.00 wt.% at 273 K, which is much higher than those of N₂ (0.51 wt.%), and CH₄ (0.58 wt.%). Hence, the above values clearly suggested that **CYCU-5** has selective CO₂ gas adsorption over N₂, and CH₄ gases at similar conditions. The selective CO₂ adsorption over the other gases for **CYCU-5** can be ascribed to the quadrupole moment of CO₂ (-1.4×10^{-39} C m²),²⁶ which induces interaction with the framework.²⁷ By fitting the CO₂ adsorption data of **CYCU-5** to the Dubinin–Radushkevich (DR) equation, the surface area was determined to be 36.4 m²g⁻¹.

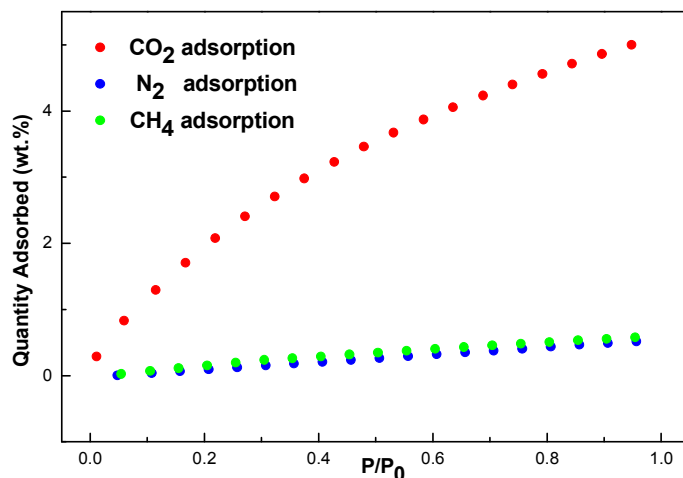


Figure 11. CO₂, N₂, and CH₄ gas uptake of CYCU-5 at 273 K.

Further, the high pressure CO₂ and CH₄ adsorption isotherms of CYCU-5 at 273 and 298 K have been measured (Figure S10, Supporting Information). The results indicated that CYCU-5 has maximum CO₂ adsorption of 94.8 cm³/g (at 33.5 bar, and 273 K) and 58.5 cm³/g (at 39.4 bar, and 298 K). However, the maximum CH₄ uptake of CYCU-5 at 89 bar pressure, is 110 cm³/g (at 273 K) and 49.9 cm³/g (at 298 K). In order to see the stability of the compounds after gas sorption experiments, PXRD was done for the compounds before and after gas sorption studies. The PXRD patterns of compounds after gas sorption studies (Figure S6, Supporting Information) indicated that the framework of all the compounds are stable after the gas sorption experiments.

Catalytic Properties

Though MOFs are well-known for their catalytic activity for various reactions, but, it is very less to explore the catalytic activity of a MOF in ring-opening polymerization (ROP) of L-Lactide (L-LA).²⁸ Hence, the catalytic activity of CYCU-5 as an initiator in ROP of L-LA has been evaluated and the representative results are outlined in Table 6. It has been noted that 78% of conversion has been observed without using toluene solvent (entry 1, Table 6). The results indicated that CYCU-5 has moderate catalytic activity for ROP of L-LA at some particular reaction conditions. Even though the catalytic activity results of CYCU-5 are not very promising, it displayed as one of the few porous MOFs having catalytic performance for ROP of L-LA.

Table 6. Results of the ROP of L-LA using compound **CYCU-5** as catalyst

Entry	$[L-LA]_0/[Cat.]_0$	Toluene (mL)	Conv. (%) ^c	M_n (calcd.) ^d	M_n (obsd.) ^e	PDI ^f
1 ^a	100/1	0	78	11278	40100 (23300)	1.70
2 ^b	100/1	5	34	4942	3900 (2262)	1.06
3 ^b	100/1	1	47	6814	15600 (9048)	1.15

^{a&b} $[Cat.]_0 = 88$ mg (0.1 mmol), 140 °C, 72 h. ^cObtained from ¹H NMR determination. ^dCalculated from the molecular weight of lactic acid times $[L-LA]_0/[Cat.]_0$ times conversion yield. ^eObtained from GPC analysis and calibrated by polystyrene standard. Values in parentheses are the values obtained from GPC times 0.56. ^fObtained from GPC analysis.

Conclusions

In summary, we have successfully synthesized six 2D metal-organic frameworks under microwave-assisted solvothermal reactions based on a rigid V-shaped 4,4'-sulfonyldibenzoic acid (H₂SBA) ligand. The compounds contain 1D open channels inside the 2D frameworks which are constructed from 1D inorganic chain SBUs. The various temperature PXRD patterns of **1-4** suggested that the de-solvated framework of **1-4** after 473 K have similar **CYCU-5** like conformation with high thermal stability. The compounds, **1-4** demonstrated the exhilarating gas adsorption about CO₂ and H₂. The gas adsorption behaviors of **CYCU-5** displayed selective CO₂ gas adsorption over N₂ and CH₄ gases at 273 K. Further, **CYCU-5** demonstrated preliminary catalytic activity on ring-opening polymerization reaction of L-Lactide.

Acknowledgments

Financial assistance received from the Ministry of Science and Technology, Taiwan (NSC 101-2113-M-033-007-MY3 and MOST 103-2632-M-033-001-MY3) is gratefully acknowledged. Acknowledgment is also made to Mrs. C.-W. Lu, Instrumentation Center, National Taiwan University, Taiwan for her help in elemental analyses.

†**Electronic supplementary information (ESI) available:** the Supporting Information file contains TGA curves and data of **1-4**, PXRD patterns at varied temperatures for **1-4**, Rietveld profile fits, the high pressure gas adsorption isotherms and tables showing selected bond lengths and H-bond lengths.

References

- (a) M. Eddaoudi, D. B. Moler, H. Li, B. Chen, T. M. Reineke, M. O'Keeffe and O. M. Yaghi, *Acc. Chem. Res.*, 2001, **34**, 319; (b) O. M. Yaghi, H. Li, C. Davis, D. Richardson and T. L. Groy, *Acc. Chem. Res.*, 1998, **31**, 474; (c) O. R. Evans and W. Lin, *Acc. Chem. Res.*, 2002, **35**, 511; (d) M. J. Zaworotko, *Chem. Commun.*, 2001, 1; (e) P. J. Hagrman, D. Hagrman and J.

- Zubieta, *Angew. Chem. Int. Ed.*, 1999, **38**, 2638; (f) M. J. Zaworotko, *Chem. Soc. Rev.*, 1994, **23**, 283; (g) M. Eddaoudi, J. Kim, N. Rosi, D. Vodak, J. Wachter, M. O'Keeffe and O. M. Yaghi, *Science*, 2002, **295**, 469; (h) R. Robson, *J. Chem. Soc. Dalton Trans.*, 2000, 3735; (i) B. Moulton and M. J. Zaworotko, *Chem. Rev.*, 2001, **101**, 1629; (j) J. L. C. Rowsell and O. M. Yaghi, *Microporous Mesoporous Mater.*, 2004, **73**, 3.
- 2 (a) O. M. Yaghi, *Access in Nanoporous Materials*, ed. T. J. Pinnavaia and M. F. Thorpe, Plenum, New York, 1995, p. 111; (b) N. Guillou, S. Pastre, C. Livage and G. Ferey, *Chem. Commun.*, 2002, 2358; (c) B. Chen, M. Eddaoudi, S. T. Hyde, M. O'Keeffe and O. M. Yaghi, *Science*, 2001, **291**, 1021; (d) N. L. Rosi, J. Eckert, M. Eddaoudi, D. T. Vodak, J. Kim, M. O'Keeffe and O. M. Yaghi, *Science*, 2003, **300**, 1127; (e) J. S. Seo, D. Whang, H. Lee, S. I. Jun, J. Oh, Y. J. Jeon and K. Kim, *Nature*, 2000, **404**, 982; (f) O. Kahn and C. Martinez, *Science*, 1998, **279**, 44; (g) J. L. C. Rowsell, A. R. Millward, K. S. Park and O. M. Yaghi, *J. Am. Chem. Soc.*, 2004, **126**, 5666. (h) W. Lin, O. R. Evans, R. Xiong and Z. Wang, *J. Am. Chem. Soc.*, 1998, **120**, 13272; (i) B. Chen, N. W. Ockwig, A. R. Millward, D. S. Contreras, O. M. Yaghi, *Angew. Chem. Int. Ed.*, 2005, **44**, 4745.
- 3 N. Stock and S. Biswas, *Chem. Rev.*, 2012, **112**, 933.
- 4 (a) H.-K. Liu, T.-H. Tsao, Y.-T. Zhang and C.-H. Lin, *CrystEngComm*, 2009, **11**, 1462; (b) X.-F. Wang, Y.-B. Zhang, H. Huang, J.-P. Zhang and X.-M. Chen, *Cryst. Growth Des.*, 2008, **8**, 4559; (c) Y.-K. Seo, G. Hundal, I. T. Jang, Y. K. Hwang, C.-H. Jun and J.-S. Chang, *Microporous Mesoporous Mater.*, 2009, **119**, 331.
- 5 (a) S. R. Batten and R. Robson, *Angew. Chem. Int. Ed.*, 1998, **37**, 1460; (b) J. Kim, B. L. Chen, T. M. Reineke, H. L. Li, M. Eddaoudi, D. B. Moler, M. O'Keeffe and O. M. Yaghi, *J. Am. Chem. Soc.*, 2001, **123**, 8239; (c) S. M. Chen, C. Z. Lu, Q. Z. Zhang, J. H. Liu and X. Y. Wu, *Eur. J. Inorg. Chem.*, 2005, 423; (d) P. M. Forster, N. Stock and A. K. Cheetham, *Angew. Chem. Int. Ed.*, 2005, **44**, 7608.
- 6 (a) V. S. S. Kumar, F. C. Pigge and N. P. Rath, *New J. Chem.*, 2004, **28**, 1192; (b) A. J. Blake, N. R. Brooks, N. R. Champness, M. Crew, A. Deveson, D. Fenske, D. H. Gregory, L. R. Hanton, P. Hubberstey and M. Schroder, *Chem. Commun.*, 2001, 1432; (c) Y. J. Qi, Y. H. Wang, C. W. Hu, M. H. Cao, L. Mao and E. B. Wang, *Inorg. Chem.*, 2003, **42**, 8519.
- 7 (a) S.-Q. Zang, Y. Su, Y.-Z. Li, H.-Z. Zhu and Q.-J. Meng, *Inorg. Chem.*, 2006, **45**, 2972; (b) L. Pan, M. B. Sander, X.-Y. Huang, J. Li, M. Smith, E. Bittner, B. Bockrath and J. K. Johnson, *J. Am. Chem. Soc.*, 2004, **126**, 1308; (c) X.-L. Wang, C. Qin, E.-B. Wang, Y.-G. Li and Z.-M. Su, *Chem. Commun.*, 2005, 5450; (d) X.-L. Wang, C. Qin, E.-B. Wang, Y.-G. Li, Z.-M. Su, L. Xu and L. Carlucci, *Angew. Chem., Int. Ed.*, 2005, **44**, 5824; (e) X. L. Wang, C. Qin, E.-B. Wang and Z.-M. Su, *Chem.-Eur. J.*, 2006, **12**, 2680; (f) A. M. Plonka, D. Banerjee, W. R. Woerner, Z. Zhang, J. Li and J. B. Parise, *Chem. Commun.*, 2013, **49**, 7055; (g) T. Kundu, S. C. Sahoo and

- R. Banerjee, *Chem. Commun.*, 2012, **48**, 4998; (h) D. Banerjee, Z. Zhang, A. M. Plonka, J. Li and J. B. Parise, *Cryst. Growth Des.*, 2012, **12**, 2162; (i) A. M. Plonka, D. Banerjee, W. R. Woerner, Z. Zhang, N. Nijem, Y. J. Chabal, J. Li, and Parise, *Angew. Chem. Int. Ed.*, 2013, **52**, 1692.
- 8 (a) C. T. Yeh, W. C. Lin, S. H. Lo, C. C. Kao, C.-H. Lin and C. C. Yang, *CrystEngComm*, 2012, **14**, 1219; (b) P.-C. Cheng, F.-S. Tseng, C.-T. Yeh, T.-G. Chang, C.-C. Kao, C.-H. Lin, W.-R. Liu, J.-S. Chen and V. Zima, *CrystEngComm*, 2012, **14**, 6812; (c) D. Senthil Raja, J.-H. Luo, C.-Y. Wu, Y.-J. Cheng, C.-T. Yeh, Y.-T. Chen, S.-H. Lo, Y.-L. Lai and C.-H. Lin, *Cryst. Growth Des.*, 2013, **13**, 3785.
- 9 (a) S. Noro, R. Kitaura, M. Kondo, S. Kitagawa, T. Ishii, H. Matsuzaka and M. Yamashita, *J. Am. Chem. Soc.*, 2002, **124**, 2568; (b) A. Kondo, H. Noguchi, L. Carlucci, D. M. Proserpio, G. Ciani, H. Kajiro, T. Ohba, H. Kanoh and K. Kaneko, *J. Am. Chem. Soc.*, 2007, **129**, 12362; (c) P. Pachfule, R. Das, P. Poddar and R. Banerjee, *Inorg. Chem.*, 2011, **50**, 3855; (d) J. Zhang, A. V. Biradar, S. Pramanik, T. J. Emge, T. Asefa and J. Li, *Chem. Commun.*, 2012, **48**, 6541. (e) S.-i. Noro, Y. IHijikata, M. nukai, T. Fukushima, S. Horike, M. Higuchi, S. Kitagawa, T. Akutagawa, T. Nakamura, *Inorg. Chem.*, 2013, **52**, 280.
- 10 (a) O. Khan, *Molecular Magnetism*, VCH: Weinheim, 1993; (b) R. L. Carlin, *Magnetochemistry*; Springer-Verlag: Berlin, Heidelberg, 1986.
- 11 (a) S. L. James, *Chem. Soc. Rev.*, 2003, **32**, 276; (b) H. C. Zhou, J. R. Long and O. M. Yaghi, *Chem. Rev.*, 2012, **112**, 673; (c) Y. Li, Z. Ju, B. Wu and D. Yuan, *Cryst. Growth Des.*, 2013, **13**, 4125.
- 12 (a) S. Shackley, D. Reiner, P. Upham, H. d. Coninck, G. Sigurthorsson and J. Anderson, *Int. J. Greenhouse Gas Control*, 2009, **3**, 344; (b) J. F. M. Orr, *Energy Environ. Sci.*, 2009, **2**, 449.
- 13 W. Zhuang, H. Sun, H. Xu, Z. Wang, S. Gao, L. Jin, *Chem. Commun.*, 2010, **46**, 4339.
- 14 C.-Y. Li, J.-K. Su, C.-J. Yu, Y.-E. Tai, C.-H. Lin and B.-T. Ko, *Inorg. Chem. Commun.*, 2012, **20**, 60.
- 15 (a) Bruker AXS, APEX2, V2010.3, Bruker AXS Inc.: Madison, WI; (b) SADABS V2008/1; SAINT+ V7.60A, Bruker AXS Inc.: Madison, WI.
- 16 (a) SHELXTL V6.14; Bruker AXS Inc., Madison, WI, 2008; (b) G. M. Sheldrick, *Acta Crystallogr.*, 2008, **A64**, 112.
- 17 A. C. Larson and R. B. Von Dreele, "General Structure Analysis System (GSAS)", Los Alamos National Laboratory Report LAUR 2000, 86-748.

18. T. Loiseau, H. Muguerra, G. Férey, M. Haouas and F. Taulelle, *J. Solid State Chem.*, 2005, **178**, 621.
19. A. L. Spek, *J. Appl. Crystallogr.*, 2003, **36**, 7.
20. P. K. Thallapally, J. Tian, M. R. Kishan, C. A. Fernandez, S. J. Dalgarno, P. B. McGrail, J. E. Warren and J. L. Atwood, *J. Am. Chem. Soc.*, 2008, **130**, 16842.
21. Z. X. Zhao, Z. Li and Y. S. Lin, *Ind. Eng. Chem. Res.*, 2009, **48**, 10015.
22. J. Y. Lee, J. Li and J. Jagiello, *J. Solid State Chem.*, 2005, **178**, 2527.
23. S. Ma, X.-S. Wang, C. D. Collier, E. S. Manis and H.-C. Zhou, *Inorg. Chem.*, 2007, **46**, 8499.
24. H. R. Moon, N. Kobayashi and M. P. Suh, *Inorg. Chem.*, 2006, **45**, 8672.
25. A. M. Shultz, O. K. Farha, J. T. Hupp and S. T. Nguyen, *J. Am. Chem. Soc.*, 2009, **131**, 4204.
26. (a) H. J. Park and M. P. Suh, *Chem. Commun.*, 2010, 610; (b) S. Couck, J. M. Denayer, G. V. Baron, T. Remy, J. Gascon and F. Kapteijin, *J. Am. Chem. Soc.*, 2009, **131**, 6326; (c) X.-R. Meng, D.-C. Zhong, L. Jiang, H.-Y. Li and T.-B. Lu, *Cryst. Growth Des.*, 2011, **11**, 2020; (d) L. Bastin, P. S. Brcia, E. J. Hurtado, J. C. Silva, A. E. Rodrigues and B. Chen, *J. Phys. Chem. C*, 2008, **112**, 1575.
27. H. S. Choi and M. P. Suh, *Angew. Chem., Int. Ed.*, 2009, **48**, 6865.
28. C. J. Chuck, M. G. Davidson, M. D. Jones, G. Kociok-Kohn, M. D. Lunn and S. Wu, *Inorg. Chem.*, 2006, **45**, 6595.

Table of Contents Synopsis

Structural transformation has been observed in porous 2D metal-organic frameworks which were synthesized under the microwave-assisted solvothermal reactions.

